VILNIUS UNIVERSITY
CENTRE FOR PHYSICAL SCIENCES AND TECHNOLOGY

JULIUS VAŽGĖLA

CHARGE CARRIER TRANSPORT AND RECOMBINATION IN BULK HETEROJUNCTIONS

Summary of doctoral dissertation
Technology Sciences, Material Engineering (08 T)

Vilnius, 2017

The doctoral dissertation was prepared in 2013 – 2017 at the Department of Solid State Electronics, Vilnius University.

Scientific supervisor – prof. habil. dr. Gytis Juška (Vilnius University, Technology Sciences, Material Engineering – 08 T).

Council of defence of the doctoral thesis:

Chairman – prof. habil. dr. Sigitas Tamulevičius (Kaunas University of Technology, Technological Sciences, Materials Engineering – 08T).

Members:

prof. habil. dr. Vidmantas Gulbinas (Center for Physical and Technology, Technology Sciences, Material Engineering – 08T);

prof. habil. dr. Karolis Kazlauskas (Vilnius University, Physical Sciences, Physics – 02P);

prof. dr. Nerija Žurauskienė (Center for Physical and Technology, Physical Sciences, Physics – 02 P);

assistant prof. habil. dr. Mihaela Girtan (University of Angers, Technology Sciences, Material Engineering – 08T).

The official defence of the doctoral thesis will be held in the public session of the Vilnius University Defence Council at 15 h on October 31, 2017, in B336 lecture room of National Center for Physical Sciences and Technology.

Adress: Saulėtekio Ave. 3 ,Vilnius, LT-10257.

The doctoral thesis is available at Vilnius University Library and at the official Vilnius University website *www.vu.lt/naujienos/ivykiu-kalendorius*.

VILNIAUS UNIVERSITETAS
FIZINIŲ IR TECHNOLOGIJOS MOKSLŲ CENTRAS

JULIUS VAŽGĖLA

KRŪVININKŲ PERNAŠA IR REKOMBINACIJA ORGANINĖSE TŪRINĖSE HETEROSANDŪROSE

Daktaro disertacijos santrauka
Technologijos mokslai, medžiagų inžinerija (08 T)

Vilnius, 2017

Disertacija rengta 2013 – 2017 metais Vilniaus universitete, Kietojo kūno elektronikos katedroje.

Mokslinis vadovas – prof. habil. dr. Gytis Juška (Vilniaus universitetas, technologijos mokslai, medžiagų inžinerija – 08 T).

Disertacija ginama viešajame disertacijos Gynimo tarybos posėdyje:

Pirmininkas – prof. habil. dr. Sigitas Tamulevičius (Kauno technologijos universitetas, technologijos mokslai, medžiagų inžinerija – 08T).

Nariai:

prof. habil. dr. Vidmantas Gulbinas (Fizinių ir technologijos mokslų centras, technologijos mokslai, medžiagų inžinerija – 08T);

dr. Karolis Kazlauskas (Vilniaus universitetas, fiziniai mokslai, fizika – 02P);

prof. dr. Nerija Žurauskienė (Fizinių ir technologijos mokslų centras, fizika – 02 P);

prof. habil. dr. Mihaela Girtan (Anžė universitetas, Prancūzija, technologijos mokslai, medžiagų inžinerija – 08T).

Disertacija bus ginama viešame disertacijos Gynimo tarybos posėdyje 2017 m. spalio mėn. 31 dieną 15 valandą Nacionaliniame fizinių ir technologijos mokslų centre B336 auditorijoje.

Adresas: Saulėtekio al. 3, Vilnius, LT-10257.

Disertacijos santrauka išsiuntinėta 2017 m. rugsėjo mėn. 12 d.

Disertaciją galima peržiūrėti Vilniaus universiteto bibliotekoje ir VU interneto svetainėje adresu: *www.vu.lt/naujienos/ivykiu-kalendorius*.

CONTENTS

Santrauka

2015 metais Paryžiuje 196 šalys patvirtino susitarimą iki 2050 m. pasiekti, kad šiltnamio efektą sukeliančių dujų būtų išmesta ne daugiau nei Žemė gali sugerti. Taigi, per 2011–2050 m. laikotarpį anglies dioksido emisija turėtų būti ne didesnė nei 1100 gigatonų [1]. Tai reiškia, kad iki 2050 m. turėtų būti neišnaudoti du trečdaliai dabartinių iškastinio kuro rezervų [2], t. y. trečdalis naftos, pusę dujų bei 80 % akmens anglies rezervų [3]. Be to, šių energijos šaltinių naudojimas nustos augti ir toliau mažės [4]. Po 2011 m. Fukušimos atominės elektrinės avarijos pasikeitė požiūris ir į atominę energetiką. Taigi, didėjančiam energijos poreikiui patenkinti vis didesnę reikšmę turės atsinaujinantys energijos šaltiniai, iš kurių saulė turi didžiausią energijos potencialą.

Pirmą kartą 1839 m. fotovoltinį efektą pastebėjo A. E. Becquerel [5]. 1954 m. Bell laboratorijoje D. M. Chapin su kolegomis sukūrė pirmąją praktišką silicinę p-n sandūros saulės celę [6]. Po metų Hoffman Electronics pradėjo pardavinėti 2 % efektyvumo celes, kurių kaina buvo 1785 USD/W [7]. Šiuo metu komercinių monokristalinių silicinių saulės celių kaina yra sumažėjusi iki 0,5 USD/W, o efektyvumas pasiekęs apie 20 %. Nors siliciniai saulės elementai yra populiariausios celės, jos turi ir keletą trūkumų: didelio grynumo silicinių plokštelių gamyba yra brangi, elementai nelankstūs, trapūs bei nepralaidūs saulės šviesai, o tai riboja jų pritaikymą nišinėse srityse. Šių trūkumų neturi organiniai tūrinės heterosandūros (angl. *Bulk Heterojunction*, BHJ) saulės elementai, kurie gali būti įvairių spalvų, dalinai permatomi, gaminami pigiu spausdinimo būdu ant lankstaus pagrindo. Dėl šių savybių jie gali būti integruojami į nešiojamus elektroninius prietaisus, naudojami kaip spalvoti, elektros energiją generuojantys langai ir t. t.

Krūvininkų fotogeneracijos, atskyrimo, pernašos bei surinkimo ties atitinkamais elektrodais efektyvumas ir rekombinacijos procesai priklauso nuo

tūrinės heterosandūros sluoksnio kompozicijos bei morfologijos. Siekiant sukurti efektyviausius tūrinės heterosandūros saulės elementus tarp kitų parametrų būtina užtikrinti ir efektyvią krūvininkų pernašą. Vieni svarbiausių dinamikos parametrų yra krūvininkų judriai ir rekombinacijos mechanizmai bei jų spartos. Šių parametrų įvertinimui naudojamos įvairios metodikos, tokios kaip lėkio trukmės (angl. *Time-of-flight*, ToF), krūvininkų ištraukimo tiesiškai kylančia įtampa (angl. *Charge Extraction by Linearly Increasing Voltage*, CELIV), fotogeneruotų (injektuotų) krūvininkų ištraukimas tiesiškai kylančia įtampa, foto-CELIV (i-CELIV). Deja, ToF tinkamas tik mažo laidumo storiems bandiniams, be to šiuo metodu įvertintos rekombinacijos spartos vertė stipriai priklauso nuo apkrovos varžos [8], CELIV tinkamas tik pagrindinių krūvininkų judrio įvertinimui, naudojant foto-CELIV galimos didelės paklaidos dėl fotogeneruotų krūvininkų pradinio pasiskirstymo ir rekombinacijos [9, 10, 11], i-CELIV judrio įvertinimo tikslumas stipriai priklauso nuo izoliatoriaus bei organinio sluoksnio talpų santykio, be to i-CELIV, taip pat kaip ir CELIV bei foto-CELIV metodu išmatuota judrio priklausomybė nuo elektrinio lauko stiprio yra apytikslė.

Šiame darbe buvo tobulinima i-CELIV metodika, pritaikytos dvi korekcijos, iš kurių pirmoji skirta tiksliam judrio įvertinimui nepriklausomai nuo izoliatoriaus bei organinio sluoksnio talpų santykio ir antroji, leidžianti atlikti tikslius judrio priklausomybės nuo elektrinio lauko stiprio matavimus. Taip pat buvo įvertintos įvairių struktūrų trikomponenčių Si-PCPDTBT:P3HT:$PC_{61}BM$ saulės elementų fotoelektrinės charakteristikos bei nustatyta efektyviausia struktūra. Taipogi foto-CELIV bei ToF metodikomis buvo tirta krūvininkų rekombinacija, parodyta, kad esant stipriai koncentruotam elektriniam laukui foto-CELIV technika galima gauti labai netikslų rekombinacijos įvertinimą.

Summary

In 2015 in Paris 196 countries approved the agreement before 2050 to make greenhouse gas emissions to no more than the Earth can absorb. Thus, during the years 2011-2050 emission of carbon dioxide should not be higher than 1100 gigatons [1]. This means that, by the year 2050 it should be unused two-thirds of current fossil fuel reserves [2], i.e. one-third of the oil, half of the gas and 80% of coal reserves [3]. Moreover, the growth of these energy sources usage will stop and continue to decline [4]. After Fukushima nuclear power plant accident in 2011 the attitude to nuclear energy has changed. Thus, the growing energy needs will be satisfied by increasingly important renewable energy sources, of which the sun has the greatest energy potential.

The photovoltaic effect was discovered in 1839 by A. E. Becquerel [5]. In 1954 in Bell laboratory D. M. Chapin and his colleagues have developed the first practical silicon p-n junction solar cell [6]. One year later, Hoffman Electronics started to sell a 2% efficiency cells for 1785 USD/W [7]. Currently, commercial monocrystalline silicon solar cell cost is reduced to 0.5 USD / W and efficiency reached 20%. Although silicon solar cells are the most popular, they have several disadvantages: the high-purity silicon wafer production is expensive, elements are rigid, brittle and opaque, which limits their application in niche areas. Organic Bulk Heterojunction (BHJ) solar cells do not posses these shortcomings. BHJ can be a variety of colors, partially transparent, cheaply printed on a flexible substrate. Due to these properties, they can be integrated into portable electronic devices, used as a colorful, electricity-generating windows and etc.

Charge carriers photogeneration, separation, transport, collection at the corresponding electrodes and the efficiency of recombination processes depend on the composition and morphology of bulk heterostructure layer. In order to obtain BHJ solar cells with maximum efficiency, among other things it is

necessary to ensure effective charge carrier transport. One of the most important parameters are charge carrier mobility and recombination mechanisms. There are several different techniques to study these processes, such as Time-of-flight (ToF), Charge Extraction by Linearly Increasing Voltage (CELIV), photogenerated (injected) Charge Extraction by Linearly Increasing Voltage (photo-CELIV (i-CELIV)). However, TOF is suitable only for low conductivity thick samples; moreover, the rate of the recombination is strongly influenced by the load resistance [8], CELIV can only be used to measure the mobility of the majority charge carriers and using photo-CELIV errors may occur due to the influence of the initial distribution and recombination of the photogenerated charge carriers [9, 10, 11], in i-CELIV technique the estimation of the transit time and herewith mobility is influenced by the ratio of semiconductor's and insulator's capacitances and by using i-CELIV as well as CELIV or photo-CELIV determination of the mobility dependence on electrical field is extremely approximate.

In this work i CELIV technique was improved and applied two correction: first one is dedicated to an accurate assessment of mobility independent of the insulator and the organic layer thicknesses ratio and the second is applied in order to perform accurate measurements of mobility dependence on electric field. It was also evaluated photovoltaic characteristics of various structures ternary Si-PCPDTBT:P3HT:$PC_{61}BM$ solar cells and found the most efficient structure. Also charge carrier recombination was studied with photo-CELIV and ToF techniques. It was demonstrated that in case of the concentrated electric field, photo-CELIV fails to evaluate the recombination rate and order from the density decay of charge carriers.

Main objectives

1. To apply i-CELIV technique for the investigation of charge carrier transport properties in bulk heterojunctions.

2. To determine the influence of composition of Si-PCPDTBT:P3HT:$PC_{61}BM$ solar cells to their photoelectric properties.

3. To estimate bimolecular recombination in organic solar cells employing different techniques.

Novelty

1. For the first time i-CELIV technique was applied for the measurements of mobility dependence on electric field to determine both, electron and hole width of Gaussian density of states (DOS); offered two corrections, necessary for mobility calculations: the first one is designed to eliminate error of measured transit time in thin films, whose capacity is comparable or higher than capacity of insulator; the second one is applied taking into account charge carrier transport at changing electric field during i-CELIV measurements.

2. It was indicated that in ternary Si-PCPDTBT:P3HT:$PC_{61}BM$ solar cells with increasing polymer Si-PCPDTBT ratio charge carrier mobility and open circuit voltage increases too but herewith recombination losses become more significant which limits the efficiency of these cells.

3. It has been shown that photo-CELIV technique measured reduced charge carrier density decay is reduced due to their spatially separation.

Contribution of the author

Author prepared all the samples for i-CELIV measurements. Most measurements and all processing of experimental results were performed by the author. Publications were mainly prepared by the author of this dissertation.

Statements to defend

1. I-CELIV technique can be used for the investigation of both, electron and hole mobility dependence on electric field.

2. With increasing ratio of polymer Si-PCPDTBT in ternary blends of Si-PCPDTBT:P3HT:$PC_{61}BM$ bimolecular recombination increases too, which limits the efficiency of these solar cells.

3. Charge carrier density decay measured by photo-CELIV technique indicates strongly reduced Langevin recombination that is caused by spatially separated charge densities of electrons and holes.

Chapter 1

Experimental details and methods

1.1. I-CELIV

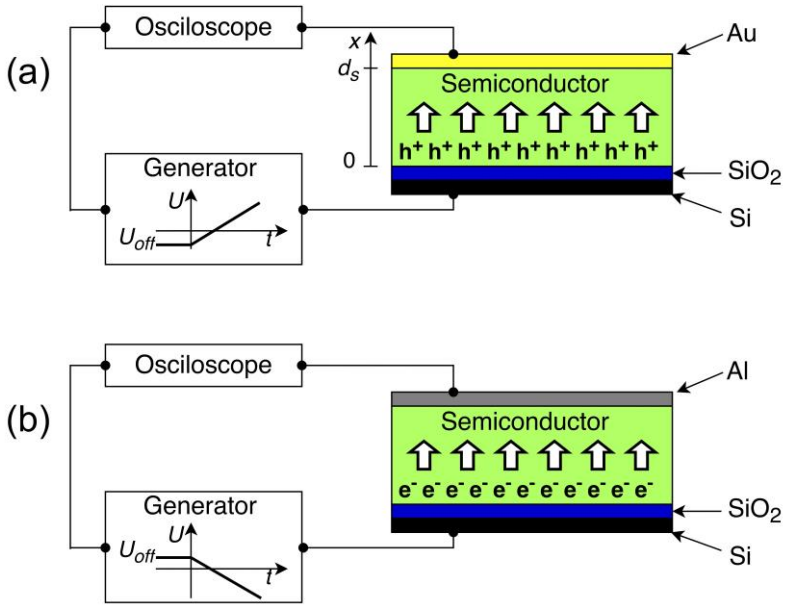

Fig. 1. The schematic view of i-CELIV experimental setups for the holes extraction (a) and electrons extraction (b).

The structures of the samples for i-CELIV measurements are shown in Fig. 1. Heavily doped silicon wafer with 270 nm thick SiO_2 layer was used as the substrate. [6,6]-Phenyl C_{61} butyric acid methyl ester ($PC_{61}BM$) and poly[2,6-(4,4-bis-(2-ethylhexyl)-4H-cyclopenta [2,1-b;3,4-b′]dithiophene)-alt-4,7(2,1,3-benzothiadiazole)] (PCPDTBT) were dissolved separately in dichlorobenzene (10 mg/ml) and 1:2, 1:1, 2:1 and 3:1 ratios mixture solutions were prepared. The solutions were heated up to 70 ^{0}C and drop casted under

nitrogen atmosphere on the substrate of silicon dioxide. Active layer thickness was in a range of 0.5–3 μm. 40 nm aluminum and 60 nm gold top electrodes were evaporated through a shadow mask under vacuum below 10^{-6} mbar.

For i-CELIV measurements a signal generator (Tektronix AFG3022B) and oscilloscope (Tektronix DPO4054B) were used. A constant negative (positive) voltage was applied to the gold (aluminum) contact for injecting holes (electrons) while linearly increasing voltage was used to extract them (Fig. 1). The shapes of current transient were used for results analysis that is overwied in Chapter 2.

1.2. Time-of-Flight

Time-of-Flight (ToF) technique were used to evaluate Langevin prefactor value ξ [12]:

$$\xi = \frac{k}{k_{\mathrm{L}}} = \frac{CU}{Q_{\mathrm{e}}}\frac{t_{\mathrm{tr}}}{t_{\mathrm{e}}}, \tag{1.1}$$

where k is the coefficient of the second-order recombination, k_{L} is Langevin recombination coefficient, $k_{\mathrm{L}} = e(\mu_{\mathrm{n}}+\mu_{\mathrm{p}})/\varepsilon\varepsilon_0$, μ_{n} (μ_{p}) – electron (hole) mobility, ε (ε_0) – relative (absolute) dielectric permittivity, t_{tr} – charge carrier transit time, $t_{\mathrm{tr}} = d^2/\mu U$, d is the thickness of the active layer, U – applied voltage, Q_{e} – extracted charge, t_{e} is extraction time – the difference between half-width of the integral mode ToF current transients at the high and low intensities of light, $t_e = t_{1/2}(L_{Qg >> CU}) - t_{1/2}(L_{Qg << CU})$ (Fig. 8), L – light intensity, Q_{g} – generated charge. It is important to mention that light intensity must be high enough to ensure saturation of ToF current transient on light intensity as it will be shown below.

1.3. HI-RPV

It is acknowledged Langevin recombination reduction coefficient ξ obtained from integral ToF strongly depends on circuit resistance [8]. Taking this into consideration, B. Philippa et al. offered a new method, High Intensity Resistance dependent Photo Voltage (HI-RPV) technique that allows recombination measurements that are independent of the experimental conditions [13]. In this technique Langevin recombination reduction coefficient ξ is used as a fitting parameter. Extracted charge Q_e depends on external resistance as follows:

$$\frac{Q_e}{CU} = 1 + p_1 \log\left[1 + p_2\left(\frac{t_{tr(sum)}}{R_{sum}C}\right)^{p_3}\right], \tag{1.2}$$

where

$$t_{tr(sum)} = d^2/U\,(\mu_h + \mu_e), \tag{1.3}$$

where $t_{tr(sum)} = d^2/U(\mu_p+\mu_e)$, μ_p (μ_n) – mobility of hole (electron), R_{sum} – complete circuit resistance, which is equal to the sum of the load resistance and the solar cell series resistance and

$$p_1 = 1.829\left(\xi + 0.0159\sqrt{\xi}\right)^{-1},$$

$$p_2 = 0.63\xi^{0.407},$$

$$p_3 = 0.55\xi^{0.0203}.$$

In HI-RPV technique ToF transients at high light intensities are measured for different load resistances. Extracted charge at each load resistance is then calculated by integrating the ToF transient. The dependence of extracted charge normalized to the charge stored on the contacts, Q_e/CU, is

plotted against $t_{tr}/R_{sum}C$ and theoretical plots are calculated using Eq. (1.2), Langevin recombination reduction coefficient ξ is obtained from the best fit with respect to the experimental values.

1.4. Photo-CELIV

The concentration decay of electrons in solar cell can be described as:

$$\frac{\mathrm{d}n}{\mathrm{d}t} = -\frac{1}{e}\frac{\mathrm{d}j_n}{\mathrm{d}x} + G - R, \tag{1.4}$$

where n is the concentration of electrons, t – time, e – elementary charge, j_n – the current of electrons, G – generation rate, R – recombination rate. In photo-CELIV experiments photogenerated charge carriers are extracted after certain delay time t_{del} (G = 0). In order to avoid the extraction of charge carriers during the delay time t_{del}, an offset voltage U_{offset} (approximately equal to the open circuit voltage U_{oc}) is applied to the sample. In this case the first member on the right side of Eq. (1.4) is almost equal to zero. Taking this into account Eq. (1.4) can be simplified to:

$$\frac{\mathrm{d}n}{\mathrm{d}t} = -R = -k_0 n^{\lambda+1}, \tag{1.5}$$

where k_0 is the recombination coeffiecient independent of charge carrier density, λ+1 – the apparent recombination order.

The integration of Eq. (1.5) gives the charge carrier density dependence on time:

$$n(t) = \left(n(0)^{-\lambda} + \lambda k_0 t\right)^{-1/\lambda}. \tag{1.6}$$

In disordered materials the recombination is commonly considered as a second-order Langevin type recombination that is limited by the probability for the electrons and holes to meet in space [14]:

$$R = k_L n^2, \tag{1.7}$$

where k_L is Langevin recombination coefficient, $k_L = e(\mu_n+\mu_p)/\varepsilon\varepsilon_0$, μ_n (μ_p) – electron (hole) mobility, ε (ε_0) – relative (absolute) dielectric permittivity. However, it was shown that in some polymer blends the recombination is reduced compared with the one predicted by Langevin [11, 13, 15, 16]. In such case the coefficient of the second-order recombination can be described as:

$$k = \xi k_L = \xi \frac{e(\mu_n + \mu_p)}{\varepsilon\varepsilon_0}, \tag{1.8}$$

where ξ is the Langevin prefactor, ξ = 1 in a pure Langevin recombination case and $\xi < 1$ if the recombination is reduced.

Photo-CELIV measurements were performed in three different setups: ordinary (I), ordinary setup with an offset voltage (II) and setup with a voltage switcher (III, Fig. 2). The measurements of the all setups were conducted with a pulsed second-harmonic 532 nm Nd:YAG laser (EKSPLA PL2143), oscilloscope (Tektronix DPO4054B) and generator (Tektronix AFG3022B). The additional generator (Tektronix AFG3022B) and a controllable voltage switcher were used for the III setup. The laser pulse duration was 30 ps and the beam diameter 6 mm. At 532 nm the absorption coefficients of the samples were $\alpha = 4.1 \cdot 10^4$ cm^{-1} and $\alpha = 1.03 \cdot 10^5$ cm^{-1}, giving $\alpha d = 0.33$ and $\alpha d = 0.82$ for 20 mg/ml and 30 mg/ml sample respectively. The sample was excited through Al contact side. The laser was synchronized with triangle (Generator II) and square (Generator I, only III setup) voltage pulse generators. In order to avoid the extraction by inserted voltage during the delay time t_{del}, an offset

voltage U_{offset} was used in II setup. During the delay time t_{del} in III setup the extraction of photogenerated charge carriers was avoided by employing a voltage switcher. The sample's contacts were disconnected from the electrical circuit and after a certain delay time t_{del} Generator I applied square voltage pulse to the controllable voltage switcher which connected the contacts to the circuit (III setup). Photogenerated charge carriers were extracted after the same delay time t_{del} by the application of a linearly increasing voltage. In case of bulk photogeneration the mobility of charge carriers can be found as [17]:

$$\mu = \frac{2d^2}{3At_{max}^2\left[1+0.36\Delta j / j(0)\right]}, \tag{1.9}$$

where A is the voltage ramp, $A = \mathrm{d}U/\mathrm{d}t$, t_{max} – the time when photo-CELIV transient reaches its maximum , $j(0)$ – the displacement current density, Δj – the extraction current density (Fig. 11a).

In a time window of $0 \leq t \leq t_p$, is CELIV pulse duration, photo-CELIV transient in a sample consists of a displacement $j(0)$ and extraction Δj current densities (Fig. 11a). Applying long enough CELIV pulse, $\Delta j = 0$ at the end of the pulse. Thus, by deducting a dark transient from the illuminated one and integrating the result of it, the extracted charge Q_e can be estimated. By changing delay time t_{del} between the laser and CELIV pulses, t_{max} increases (charge carrier mobility decreases, Eq. (1.9)) and the extracted charge Q_e decreases due to the recombination. Hence, the mobility and carrier density dependences on time ($\mu(t)$ and $n(t)$ respectively), where t is the delay time t_{del}, can be measured [18]. Using the measured mobility dependence on time $\mu(t_{del})$, Eq. (1.8) and (1.6) and the recombination order of 2 ($\lambda = 1$), the decay $n(t_{del})$ of charge carrier density can be calculated employing the different values of Langevin prefactor ξ. These theoretically calculated $n(t_{del})$ trends are compared with the measured $n(t_{del})$ decay. Langevin prefactor ξ can be found from the theoretically calculated $n(t_{del})$ curve that matches experimental $n(t_{del})$ results the best.

Using photo-CELIV technique Langevin prefactor ξ can be found in a different way. If the recombination is of Langevin type, the recombination is fast and the extraction current density Δj does not exceed the displacement current density $j(0)$ (Fig. 11b) even at the saturation light intensity [19]. If the recombination is reduced ($\xi < 1$ in Eq. (1.8)), Δj exceeds $j(0)$ and saturates with

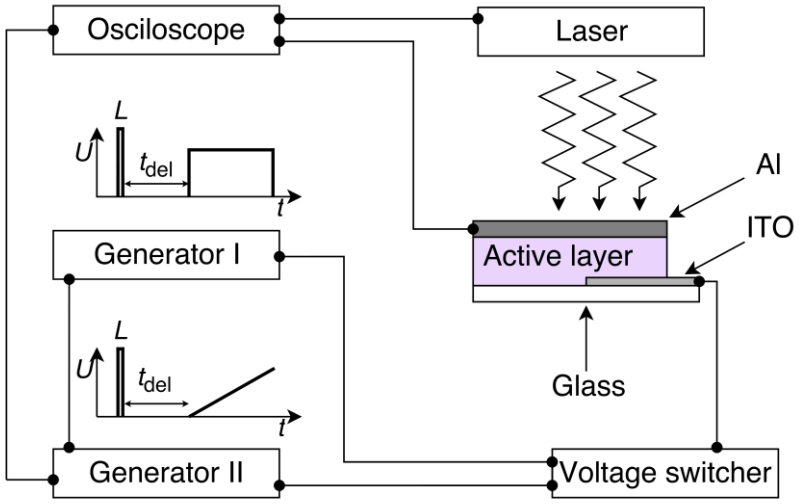

Fig. 2. The schematic view of photo-CELIV experimental setup with a voltage switcher for the investigation of charge carrier recombination.

L. From $j(0)/\Delta j$ ratio at a high light intensity Langevin prefactor ξ can be evaluated [9]:

$$\xi = \frac{k}{k_{\mathrm{L}}} = \frac{j(0)}{\Delta j}. \qquad (1.10)$$

Chapter 2

i-CELIV technique for investigation of charge carriers transport properties

There are several different techniques to measure the mobility in organic solar cells, such as time-of-flight (ToF), charge extraction by linearly increasing voltage (CELIV) and photo-CELIV [20]. However, ToF is suitable only for low conductivity thick samples, CELIV can only be used to measure the mobility of the majority charge carriers and using photo-CELIV errors may occur due to the influence of the initial distribution and recombination of the photogenerated charge carriers [9, 10, 11]. Moreover, those techniques do not allow to separate movement of holes from electrons in thin films. The injection-CELIV (i-CELIV) is a technique that overcomes previously mentioned disadvantages. Since it is rather a new method, there are several drawbacks. First, the estimation of transit time is influenced by the ratio of semiconductor's and insulator's capacitances, which could lead to errors in mobility estimation. Second, by using i-CELIV as well as CELIV or photo-CELIV determination of the mobility dependence on electrical field is extremely approximate. Here, we demonstrate how the exact values of the mobility could be obtained and the mobility dependence on electric field $\mu(E)$ could be established.

In metal-insulator-semiconductor (MIS) structure when negative (positive) offset voltage U_{off} is applied to bottom electrode (in our case heavily doped silicon), the holes (electrons) will be injected from the top Au (Al) electrode to the organic layer and will accumulate near the semiconductor-insulator interface (see Fig. 1). The distribution of the holes (or electrons) could be described as [15]:

$$p(x) = p(0)\left(1 + \frac{eU_{\text{off}}x}{2kTd_{\text{i}}}\right)^{-2}, \tag{2.1}$$

where d_{i} is the thickness of the insulator.

In the case when $eU_{\text{off}} >> kT$, charge carriers will concentrate near the insulator-semiconductor interface. The amount of charge carriers in reservoir could be estimated by extracting them with a voltage ramp $A = \mathrm{d}U/\mathrm{d}t$. The transient of the extraction current of the holes will be:

$$j(t) = e\mu p(x,t)F(x,t) + \varepsilon_{\text{s}}\varepsilon_0 \,\mathrm{d}F(x,t)/\mathrm{d}t, \tag{2.2}$$

where μ is the mobility of injected charge carriers (holes), F – electrical field in the semiconductor, ε_{s} – the dielectric constant of the semiconductor and ε_0 – an absolute dielectric permittivity.

When the capacity of the insulator C_i is much higher than the capacity of the semiconductor C_{s}, the accumulated amount of the charge $Q > CU_{\text{off}}$ (C – capacitance of MIS structure) and the boundary condition $E(0,0) = 0$ is valid. The averaging of the extraction current on coordinate from 0 till d_{s} (d_{s} – the thickness of the semiconductor, see Fig. 1a) at $t<t_{sc}$ (t_{sc} – time needed for charge carriers to reach electrode) reveals:

$$j(t) = \frac{\varepsilon_{\text{s}}\varepsilon_0 A}{d_{\text{s}}} + \frac{\varepsilon_{\text{s}}\varepsilon_0\mu}{2d_{\text{s}}}E^2(d_{\text{s}},t) = \varepsilon_{\text{s}}\varepsilon_0\frac{\mathrm{d}E(d_{\text{s}},t)}{\mathrm{d}t}. \tag{2.3}$$

Solving Eq. (2.3) gives electric field at the beginning of the package of charge carriers which is the same as at the end of the sample at d_{s}:

$$E(d_{\text{s}},t) = \sqrt{\frac{2A}{\mu}}\tan\left(\frac{t}{t_{\text{tr}}}\right) = \frac{At_{\text{tr}}}{d_{\text{s}}}\tan\left(\frac{t}{t_{\text{tr}}}\right), \tag{2.4}$$

and:

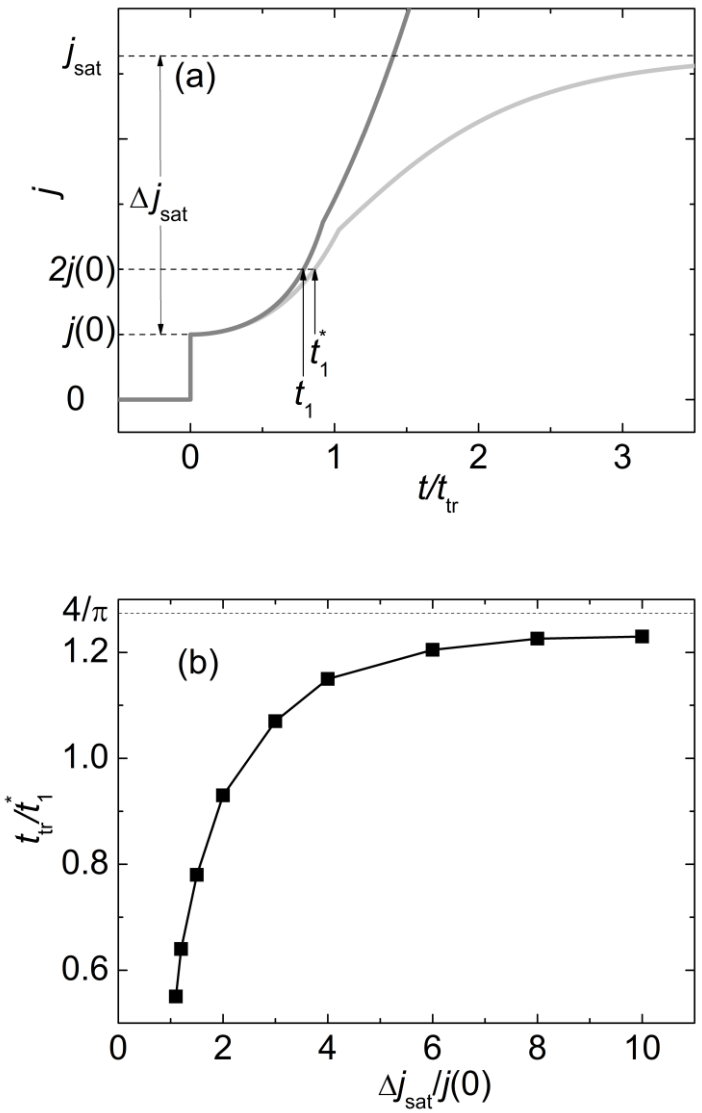

Fig. 3. Theoretically calculated i-CELIV transient's shape using Eq. (2.5) and (2.11) (dark grey line) and with evaluated saturation (light grey line) (a). Transit time t_{tr} calculation taking into account extraction current saturation (b).

$$j(t) = j(0) + \Delta j(t) = \frac{\varepsilon_s \varepsilon_0 A}{d_s}\left(1 + \tan^2\left(\frac{t}{t_{tr}}\right)\right), \qquad (2.5)$$

where $j(0)$ – the density of the displacement current (Fig. 2a), Δj – the density of the extraction current, t_{tr} is the transit time of the small charge in the case of linearly increasing voltage $t_{tr} = d_s\sqrt{\frac{2}{\mu A}}$. Since $Q > CU$, therefore current is space charge limited (SCLC) and $t_{sc} = 0.92 t_{tr}$.

Usually in the organic materials we have Poole-Frenkel type mobility dependence on electrical field, which could be simplified to $\mu(E) = \mu_0 + cE^{\gamma}$. Using $\int_0^{t_{tr}} \mu(E)E(t)\,\mathrm{d}t = d_s$, where $E(t) = At/d_s$, in case of low electric field we get:

$$t_{tr} \sim A^{-\frac{1}{2}},$$

and

$$\mu = \frac{2d_s^2}{At_{tr}^2}.$$

In case of high electric field:

$$t_{tr} \sim A^{-(\gamma+1)/(\gamma+2)} = A^{-k}, \tag{2.6}$$

and

$$\mu = \frac{(\gamma+2)d_s^2}{At_{tr}^2}. \tag{2.7}$$

In most cases the kink of the current transient near t_{sc} is hardly seen due to the diffusion of the charge carriers and stochastic nature of the transport, so the most convenient way to estimate the mobility is by using time t_1 when $\Delta j = j(0)$ (see Fig. 3a):

$$t_1 = \frac{\pi}{4}t_{tr}. \tag{2.8}$$

Inserting (2.8) into (2.4) gives:

$$F(d_S, t_1) = \frac{4}{\pi}\frac{At_1}{d_s}. \tag{2.9}$$

When the capacitances C_i and C_s are comparable, additional corrections for the estimation of transit time are needed. First, the part of the applied voltage will drop onto the insulator and carriers will drift shorter:

$$t_{tr} = d_S \sqrt{\frac{2}{\mu A}\left(1+\frac{\varepsilon_S d_i}{\varepsilon_i d_S}\right)}, \tag{2.10}$$

where ε_i is relative dielectric permittivity of the insulator.

Second, the electric field distribution kinetics will also require a supplementary correction. When $t >> t_{tr}$, the current will grow according to:

$$\frac{\Delta j(t)}{j(0)} = \frac{9}{4}\frac{t^2}{t_{tr}^2}. \tag{2.11}$$

However, the extraction current will never exceed the charging current of the insulator's capacitance C_i (see Fig. 3a) and the current density will saturate at [15]:

$$j_{sat} = \varepsilon_i \varepsilon_0 A / d_i. \tag{2.12}$$

Due to the saturation of the extraction current density, the current will grow slower than theoretical one. The lower the ratio is between the saturation current density Δj_{sat} and initial current density step $j(0)$, the larger the correction is needed. This is why instead of using Eq. (2.8), t_{tr} must be found using correction obtained by the simulation shown in Fig. 3b. So, if the condition

$$\frac{\Delta j_{sat}}{j(0)} = \frac{C_i}{C_s} = \frac{\varepsilon_i d_s}{\varepsilon_s d_i} > 1 \tag{2.13}$$

is fulfilled, charge carriers mobility at electric field

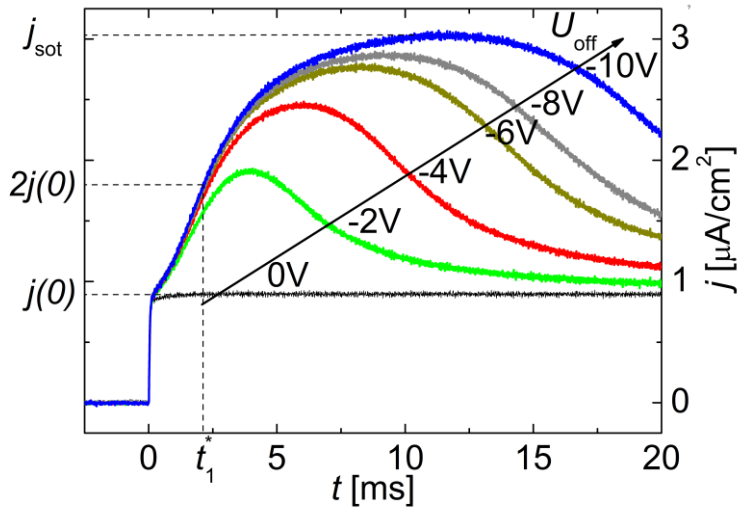

Fig. 4. Si/SiO_2/PCPDTBT/Au structure's i-CELIV extraction current transients for the $A = 2.5 \cdot 10^4$ V/s at different applied U_{off} voltage.

$$F(d_s, t_{tr}) = \frac{At_{tr}}{d_s\left(1+\frac{j(0)}{\Delta j_{sat}}\right)} \tag{2.14}$$

can be found:

$$\mu = \frac{(\gamma+2)d_s^2}{At_{tr}^2}\left(1+\frac{j(0)}{\Delta j_{sat}}\right). \tag{2.15}$$

By changing the triangle voltage pulse duration in i-CELIV technique, $\underline{A}t_{tr}$, and herewith $F(d_s, t_{tr})$ changes, and as a result, the mobility dependence on electric field can be established.

I-CELIV current transient consists of the displacement current density j_0 and the extraction current density Δj. To reach SCLC regime and the saturation of the extraction current which represents the thickness of the insulator (Eq. (2.12)), large U_{off} voltage (-10 V) was applied (Fig. 4). $\Delta j_{sat}/j(0)$ ratio is independent of voltage slope and was used for the calculation of corrected transit time (Fig. 3b).

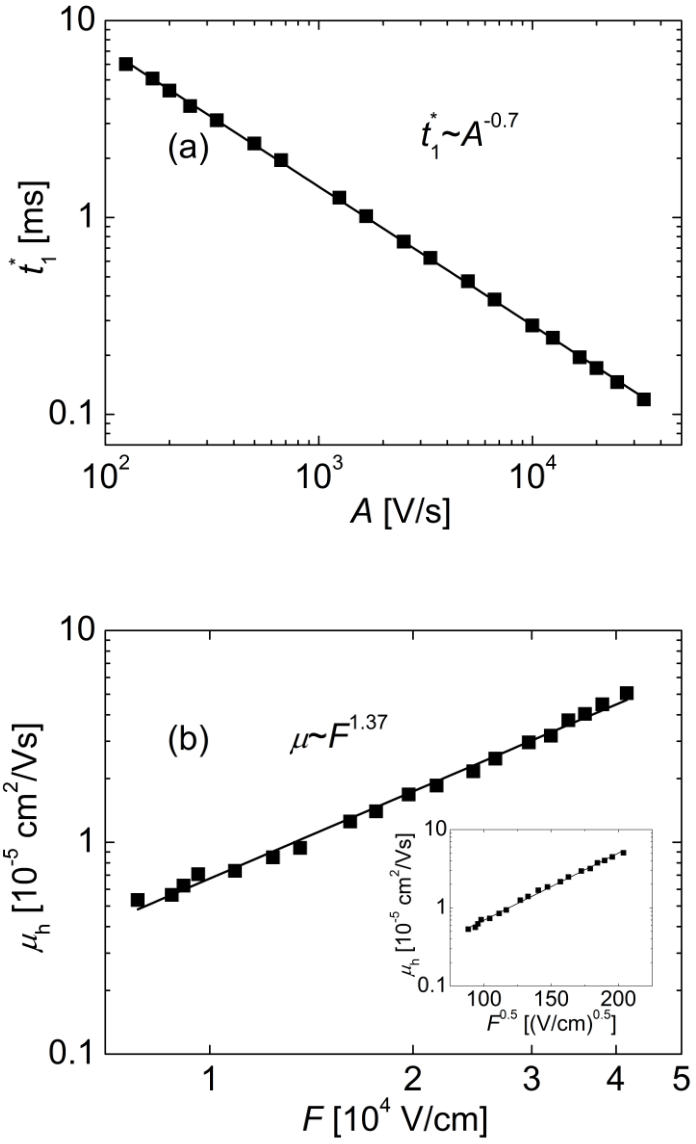

Fig. 5. Experimentally measured t_1^* dependence on voltage rising speed A (a) and hole mobility dependence on electric field in Si/SiO_2/PCPDTBT/Au structure calculated using correction (b). Inset shows mobility dependence on electric field in Poole-Frenkel coordinates.

In a pure PCPDTBT polymer measured $t_1^*(A)$ dependence indicates that the mobility of the holes is electric field dependent (Fig. 5a). By employing Eq. (2.6) it was obtained that $\mu \sim E^{1.37}$. For the calculation of the exact values of mobility Eq. (2.14) and (2.15) were used (Fig. 5b). The calculated mobility values are 2.3 times higher than estimated without any corrections.

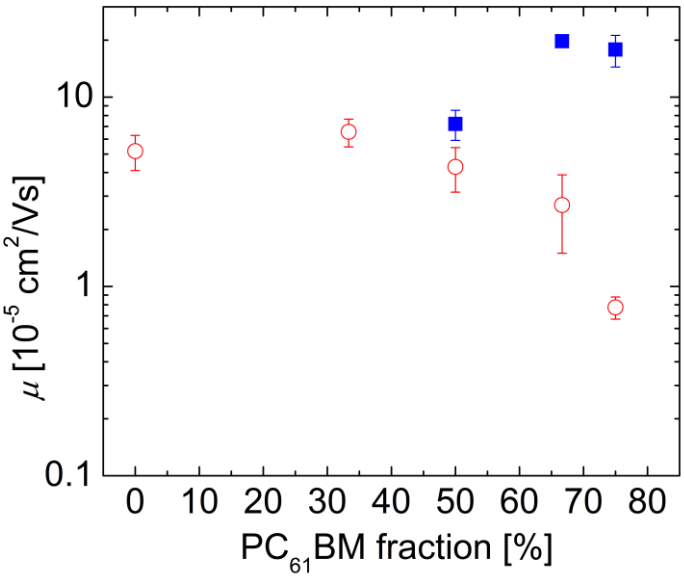

Fig. 6. $PC_{61}BM$:PCPDTBT blends electron (closed blue squares) and hole (open red circles) mobility at 4·104 V/cm electric field.

The measured mobilities of the holes and electrons in $PC_{61}BM$:PCPDTBT samples at $4 \cdot 10^4$ V/cm electric field are given in Fig. 6. In all samples electric field dependent mobility was observed for electrons and holes.

It has been demonstrated that in i-CELIV method the mobilities of the holes and electrons and their dependences on electrical field could be established by changing linearly increasing voltage pulse duration. The mobilities of the electrons and holes are electric field dependent in $PC_{61}BM$:PCPDTBT bulk heterojunctions. Using t_1^* transit time calculations can cause certain errors in mobility evaluation in i-CELIV technique. These inaccuracies can be eliminated to a certain extent by performing necessary corrections of t_1^*.

Chapter 3

Charge Carrier Transport Properties in a Ternary Silole-Based Polymer:P3HT:$PC_{61}BM$ Solar Cells

Bimolecular recombination in low mobility disordered organic materials is expected to follow Lagevin's theory which predicts a recombination rate directly proportional to the mobility of charge carriers. Most BHJ solar cells exhibit Langevin-like recombination ($\xi \approx 1$). However, few blends like the widely studied P3HT:$PC_{61}BM$ exhibit highly reduced Langevin recombination ($\xi << 1$) [11, 16, 21], which is considered a pre-requisite to relatively thick active layers (> 200 nm). Due to bimolecular recombination losses, the thickness of most high efficiency organic solar cells is confined to 60–110 nm, which limits the light absorption and hence short circuit current [22]. Typically, annealed P3HT:$PC_{61}BM$ solar cells exhibit strongly reduced Langevin recombination owing to their highly ordered morphology [23]. Ternary blends consisting of two donor moieties and one acceptor is a stimulating concept in order to enhance the optical absorption and spectral sensitivity of active layer blends [24]. The morphology of the resulting system and hence the bimolecular recombination losses largely affects the photovoltaic performance of such systems [12]. Unlike the P3HT:$PC_{61}BM$ system, the majority of low bandgap polymers exhibit Langevin type recombination when blended with $PC_{61}BM$ [25]. Therefore, while the addition of low bandgap polymers to the P3HT:$PC_{61}BM$ system improves the absorption on one hand, it can also disrupt the highly ordered morphology of P3HT:$PC_{61}BM$ blend. In this chapter we use the low bandgap polymer

poly[2,6-(4,4-bis(2-ethylhexyl)dithieno[3,2-b:2,3-d]silole)-alt-4,7-(2,1,3 benzothiadiazole)] (Si-PCPDTBT) to provide ternary blends of Si-PCPDTBT:P3HT:PCBM with improved light absorption.

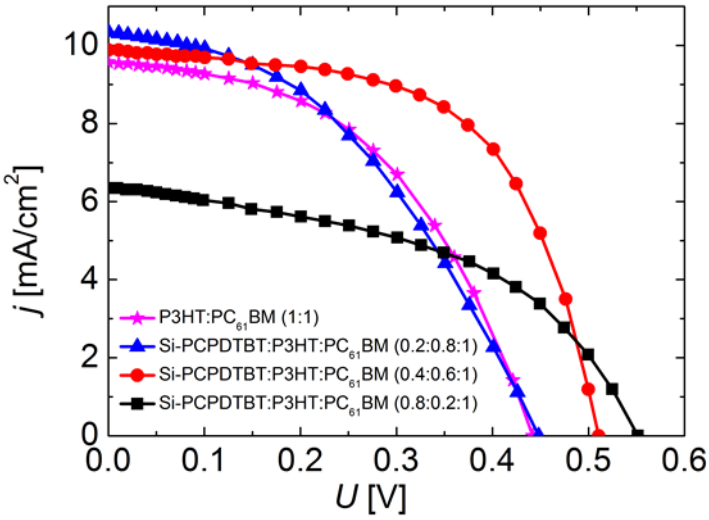

Fig. 7. Current-voltage characteristics of P3HT:$PCB_{61}M$ and representative ternary Si:PCPDTBT:P3HT:$PC_{61}BM$ solar cells under illumination of AM1.5 spectra.

Fig. 7 shows the current-voltage characteristics of solar cell devices consisting of active layers of different compositions of Si-PCPDTBT:P3HT: $PC_{61}BM$. Open-circuit voltage (U_{oc}), short circuit current density (J_{sc}) and calculated fill factor (FF) together with the power conversion efficiency (PCE) are presented in Table 1. Maximum efficiencies were obtained from blends consisting of 40% donor loading of Si-PCPDTBT, i.e, a ratio of 0.4:0.6:1 for Si-PCPDTBT:P3HT: $PC_{61}BM$, respectively. An increase in U_{oc} is observed with increasing Si-PCPDTBT content of the blends, which could be originating from the lower lying HOMO levels of Si-PCPDTBT with respect to P3HT [26]. The short circuit currents are found to increase initially with 20% donor loading of Si-PCPDTBT, i.e, a ratio of 0.4:0.6:1, respectively, for Si-PCPDTBT:P3HT: $PC_{61}BM$; which then reduces with further increase in Si-PCPDTBT content.

Table 1. Photovoltaic performance and photo-CELIV mobilities of Si-PCPDTBT:P3HT:$PC_{61}BM$ solar cells with varying composition.

Sample	U_{oc} [mV]	J_{sc} [mA/cm^2]	FF [%]	PCE [%]	R_s [Ωcm^2]	μ_{fast} [10^{-5} cm^2/Vs]	μ_{slow} [10^{-6} cm^2/Vs]
0:1:1	440	9.55	48	1.6	14.3	5.3	3.5
0.2:0.8:1	450	10.33	42	1.5	19.7	6.5	
0.4:0.6:1	510	9.85	59	2.3	9.2	6.8	
0.8:0.2:1	550	6.34	47	1.3	22.4	20	

In photo-CELIV transient of P3HT:$PC_{61}BM$ blend the maximum and the kink were observed. The positions of the maximum and kink were used for calculations of faster μ_{fast} and slower μ_{slow} charge carriers mobilities respectively (Table 1) [27].

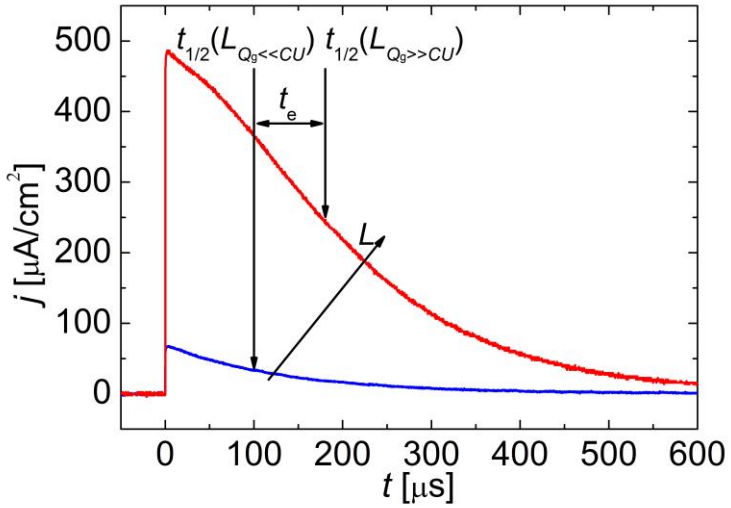

Fig. 8. Si-PCPDTBT:P3HT:$PC_{61}BM$ 0.4:0.6:1 sample's ToF transients for the U=1.5 V, R=1 kΩ at low (blue line) and high (red line) light intensities.

To study the bimolecular recombination in these blends, integral TOF measurements were carried out at high light intensities and Langevin reduction factor ξ was estimated in each of the samples using Eq. (1.1). Fig. 8 shows representative integral TOF transients and describes the estimation of extraction time t_e. Calculated ξ is shown in Fig. 8.

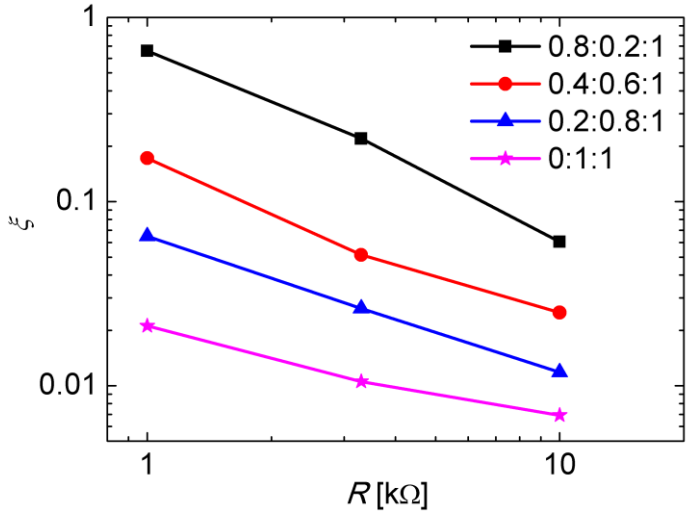

Fig. 9. Langevin recombination reduction factor ξ dependence on load resistance in Si-PCPDTBT:P3HT:$PC_{61}BM$ blends obtained by using integral ToF technique (black squares for 0:1:1, red circles for 0.4:0.6:1, blue triangles for 0.2:0.8:1 and purple stars for 0.8:0.2:1 structure respectively).

However, in case of bulk photogeneration ($\alpha d \approx 1$, which is the case in this study) the value of Langevin recombination reduction factor ξ, obtained from this technique, is acknowledged to be dependent on load resistance and is only approximate [8].

To overcome this inaccuracy we have used HI-RPV method and measured TOF transients at high light intensity ($L_{Qg} >> CU$) in ternary blends with circuit resistance in the range from 13 Ω to 1 MΩ. The dependence of normalized extracted charge Q_e/CU on normalized resistance $RC/t_{tr(sum)}$ is shown in Fig. 10. Langevin recombination reduction coefficient was used as a fitting parameter. We can see that with increasing Si-PCPDTBT ratio Langevin recombination reduction coefficient ξ increases and recombination increases significantly in blends containing relatively high contents of Si-PCPDTBT. This effect may lead to reduction in short circuit current (Table 1).

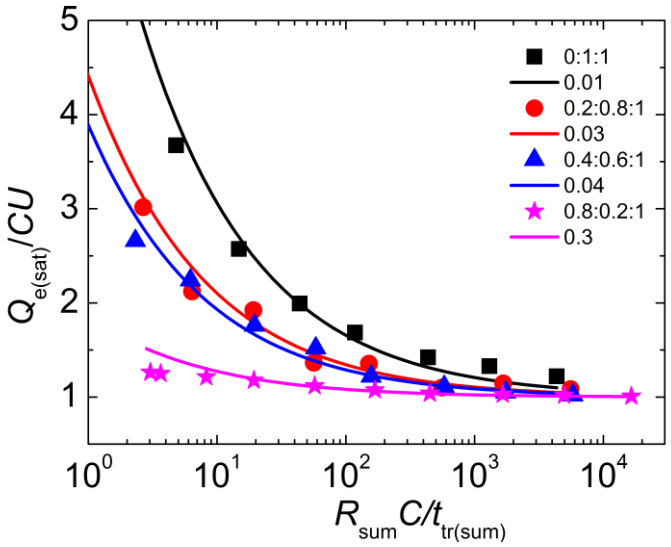

Fig. 10. Extracted charge dependence on circuit resistance in Si-PCPDTBT:P3HT:PCBM blends obtained by using HI-RPV technique (black squares for 0:1:1, red circles for 0.2:0.8:1, blue triangle for 0.4:0.6:1 and purple stars for 0.8:0.2:1 structure respectively) and theoretically calculated extracted charge dependence on circuit resistance employing Eq. (3), modeled using different Langevin recombination reduction coefficient values (black line for 0.01, red line for 0.03, blue line for 0.04 and purple line for 0.3 respectively).

The photovoltaic performance and charge transport parameters of ternary blends of Si-PCPDTBT:P3HT:$PC_{61}BM$ with different compositions has been documented. While the open circuit voltage as well as the photo-CELIV mobility of charge carriers were found to be increasing with increasing Si-PCPDTBT content, the bimolecular recombination losses were also found to be enhanced in blends with higher ratios of Si-PCPDTBT.

Chapter 4

Mismatch of bimolecular recombination in polymer TQ1/fullerene blends employing different techniques

In disordered materials the recombination is commonly considered as a second-order Langevin type recombination that is limited by the probability for the electrons and holes to meet in space [14]. Nonetheless, experimental results [28, 29], and theoretical simulations [30, 31] indicate the recombination with the order higher than 2. One of the explanations is related to the dependence of non-geminate recombination rate along with the mobility on charge carrier density. This dependence has been assigned to the presence of an energetic tail of localized trap sites [29]:

$$R = k(n)n^2 = k_0 n^{2+\delta}, \tag{4.1}$$

$$\mu(n) = \mu_0 n^{\delta}, \tag{4.2}$$

where μ_0 is a constant, δ – constant, $\delta > 0$. In disordered organic materials charge transport is explained by charge carrier hopping between localized states of the density of states. With increasing disorder the mobility becomes more dependent on charge carrier density (constant d increases). It was shown that in P3HT:PC_{61}BM blend the recombination order is 2 in case P3HT is completely crystalline (a single crystal) and with the increasing fraction of amorphous phase the concentration of traps and trapped charges increases along with the recombination order, connected to a trap-assisted recombination [32].

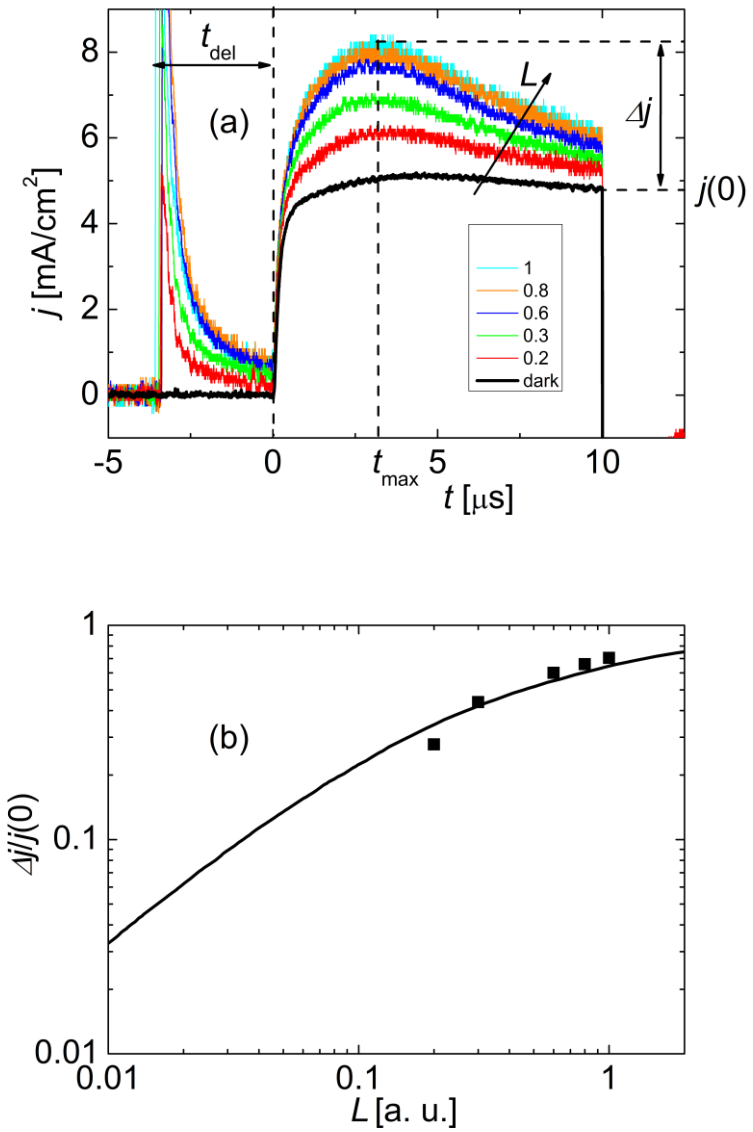

Fig. 11. pav. TQ1:$PC_{61}BM$:$PC_{71}BM$ 5:8:2 20 mg/ml sample's photo-CELIV transients for the $A = 2 \cdot 10^5$ V/s, t_{del} = 3.5 μs at a different light intensity L (arbitrary units) measured with an ordinary setup (a). The comparison between experimentally measured (squares) and theoretically calculated (line) [19] dependence of $\Delta j/j(0)$ ratio on light intensity L, where Δj and $j(0)$ are the densities of extraction and displacement current respectively (b).

Another explanation of the recombination order being higher than 2 in bulk heterojunction is related to donoreacceptor phase separation [33]. Due to the phase separation trapped charge carrier cannot recombine with the different type of charge carrier. The recombination occurs only when trapped charge

carrier becomes mobile and meets a mobile charge carrier which is oppositely charged. To sum up, in the presence of charge carrier trapping, the recombination order can be higher than 2 due to the mobility dependence on the charge carrier density and the separation of donoreacceptor phase.

In order to evaluate Langevin prefactor ξ, TQ1:$PC_{61}BM$:$PC_{71}BM$ sample was measured with an ordinary photo-CELIV technique using 2 V amplitude and 10 μs duration triangle voltage pulse. In Fig. 11a depicted photo-CELIV current transients at different laser intensity L. With increasing L due to the fast recombination, the extraction current Δj saturates to the displacement current $j(0)$ Fig. 11b. It is an explicit evidence of non-reduced Lagevin recombination (Eq. (1.10)).

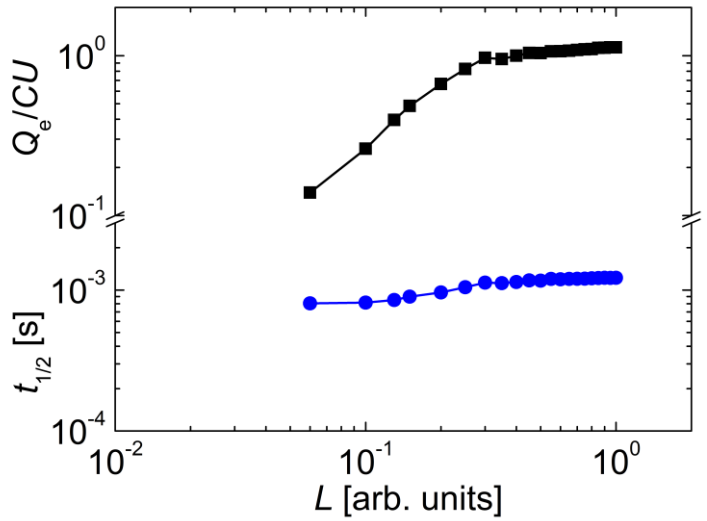

Fig. 12. Extracted charge Q_e (black squares) and extraction half-time $t_{1/2}$ (blue circles) dependence on light intensity measured with integral mode ToF technique in TQ1:$PC_{61}BM$:$PC_{71}BM$ 5:8:2 20 mg/ml sample for the $E = 2.5 \cdot 10^5$ V/cm, $R = 1$ MΩ.

Integral ToF measurements were performed additionally to assure that the recombination is of non-reduced Langevin type. The sample was excited at different light intensities L; the time $t_{1/2}$ and the extracted charge Q_e were evaluated from the current transient. From Fig. 3 it is obvious that $t_{1/2}$, the time

when ToF transient decreases twice, slightly depends on light intensity L. With increasing L, $t_{1/2}$ increases only slightly and the extracted charge Q_e saturates to CU. It shows that due to fast non-reduced Langevin recombination, no charge carrier reservoir is created [34].

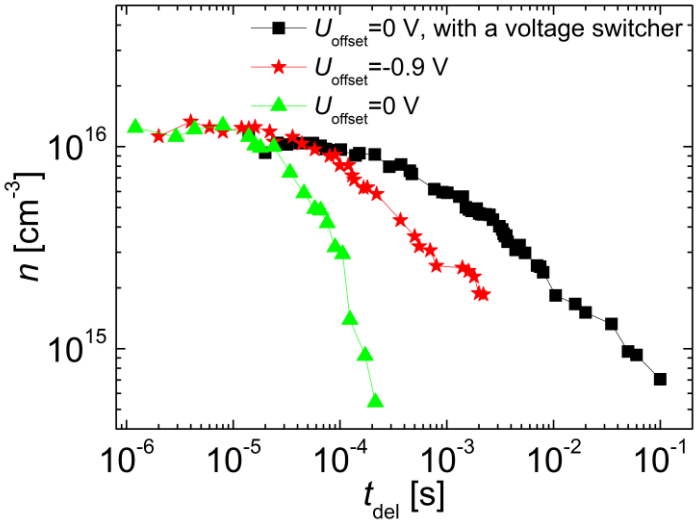

Fig. 13. Extracted charge carrier density dependences on delay time between the laser pulse and voltage ramp measured in TQ1:$PC_{61}BM$:$PC_{71}BM$ 5:8:2 30 mg/ml sample using different photo-CELIV setups: ordinary setup (green triangles), ordinary setup with an offset voltage (red stars), setup with a voltage switcher (black squares). CELIV pulse with a voltage ramp of 200 V/s was used.

We have also employed photo-CELIV technique to analyse the charge carrier density decay which gives valuable insights about the order and the rate of recombination. During photo-CELIV delay time t_{del} it is common to use offset voltage U_{offset} for the investigation of recombination processes. We can see from Fig. 13 that the employment of an offset voltage U_{offset} increases the lifetime of charge carriers. However, during the delay time even applying a large U_{offset} (-0.9 V) we observed the extraction of photogenerated charge carriers caused by a not fully compensated internal electric field. It was impossible to use a larger U_{offset} due to the commenced injection of charge carriers. Thus, when U_{offset} = -0.9 V, the charge carrier density n decreased due

to the recombination and extraction. In order to avoid this extraction, the voltage switcher was used (Fig. 13).

Employing ordinary setup photo-CELIV and Eq. (1.9), the mobility dependence on delay time $\mu(t_{del})$ was evaluated (Fig. 14, black circles) and it has a slope of 0.14. It is clearly seen that the mobility is almost time-independent and thus trapping of charge carriers is obscure. Using Eq. (1.8), Eq. (1.6) and time-independent mobility, we calculated the decay of carrier density $n(t)$ for the non-reduced ($\xi = 1$) second-order Langevin recombination (Fig. 14, black line). Taking $\mu(t_{del})$ dependence into account, it gives the recombination order of 2.14 (Fig. 14, blue line). Thus, $\mu(t_{del})$ slightly increases the recombination order compared to the time (or carrier density) independent recombination. However, we can see that the recombination is much slower than Langevin using III photo-CELIV setup (Fig. 14, grey squares). We fitted the carrier density decay with $\xi = 0.0025$ second order recombination employing Eq. (1.8) and Eq. (1.6) (Fig. 14, red line). Strongly reduced Langevin recombination contradicts the previous photo-CELIV (Fig. 11) and ToF (Fig. 12) results. The reduced Langevin type recombination was explained by the separation of the electron and hole pathways (i) [35], the limitation of the minimum mobility (ii) [36], the extent of charge delocalization of opposite charges in a charge transfer (CT) state (iii) [16] or the discrepancy between the spatially dependent nongeminate recombination rate, proportional to the local product of electron and hole densities and the recombination rate based on the average concentrations of charge carrier (iv) [11]. The (i), (ii) and (iii) explanations are related to the morphology and are not able to define the non-reduced Langevin recombination observed in the results of photo-CELIV and ToF. Thus, the reduction of the recombination rate compared with Langevin could be explained by spatially separated holes and electrons during the photo-CELIV delay time tdel. Consequently, carrier density decay $n(t)$ is strongly reduced.

While in a time range of μs-ms reduced Langevin recombination can explain an experimentally observed decay of charge carrier, it fails to define

the third-order decay in ms timescale. It was shown that in systems with a partial phase separation, trapped charge carriers can be protected from the recombination. Therefore, it increases the order of recombination [33]. As it was mentioned before, indicated pure Langevin recombination denies the morphological phase separation. However, due to the spatial separation, trapped electrons in an electron-rich region (near the cathode) and trapped holes in a hole-rich region (near the anode) are protected from the recombination and it could lead to the increased third-order recombination.

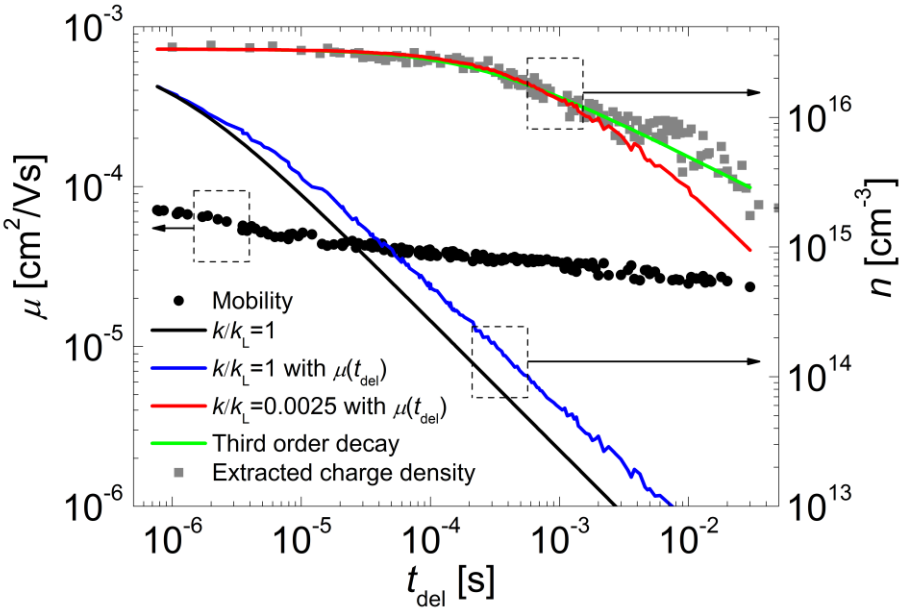

Fig. 14. Experimentally measured mobility (black circles) of TQ1:$PC_{61}BM$:$PC_{71}BM$ 5:8:2 20 mg/ml sample using photo-CELIV setup with U_{offset} = 0 V, $A = 2 \cdot 10^5$ V/s; extracted charge density dependence on delay time using photo-CELIV technique with a voltage switcher (grey squares) with A = 400 V/s and calculated charge density decay using measured time-dependent mobility in case of non-reduced (blue line) and reduced with ξ = 0.0025 (red line) Langevin recombination. Additionally, the charge carrier decay dependence on time was calculated using time-independent mobility for non-reduced Langevin (black line) and the third-order recombination with the coefficient of $k = 2 \cdot 10^{-30}$ cm^6/s (green line).

The shape of standard setup photo-CELIV and the results of ToF experiments confirm the non-reduced Langevin recombination of the second-order in TQ1:$PC_{61}BM$:$PC_{71}BM$ blends. The recombination processes were also investigated by photo-CELIV technique from charge carrier density decay. However, in case of the concentrated electric field at the contacts, the density of photogenerated charge carrier decreases due to both the recombination and the extraction by the internal electric field in standard photo-CELIV setup even with applied offset voltage. A voltage switcher that disconnects sample's contacts from the electrical circuit during delay time can also be used in order to avoid the charge carrier extraction. Employing photo-CELIV setup with a voltage switcher, the decay of the charge carrier density was measured, and it shows the non-geminate strongly reduced recombination of the thirdorder. Due to the concentrated electric field, the electrons are concentrated at the cathode and the holes – at the anode. This leads to the spatially dependent recombination rate that is proportional to the local product of electron and hole concentrations and this recombination is strongly reduced compared to Langevin recombination. To sum up, in case of the concentrated electric field, photo-CELIV fails to evaluate the recombination rate and order from the density decay of charge carriers.

Conclusions

1. I-CELIV technique can be used for measurements of both, hole and electron mobility dependence on electric field.

2. While the open circuit voltage as well as the photo-CELIV mobility of charge carriers were found to be increasing with increasing Si-PCPDTBT content in Si-PCPDTBT:P3HT:$PC_{61}BM$ bulk heterojunction, the bimolecular recombination losses were also found to be enhanced in the blends with higher ratios of Si-PCPDTBT. Thus, it was found that the composition of the most effective structure is 0.4:0.6:1.

3. Photo-CELIV technique measured charge carrier density decay is reduced due to their spatially separation.

References

[1] M. Meinshausen, N. Meinshausen, W. Hare, S. C. B. Raper, K. Frieler, R. Knutti, D. J. Frame, and M. R. Allen, Nature **458**, 1158–1162 (2009).

[2] M. R. Raupach, S. J. Davis, G. P. Peters, R. M. Andrew, J. G. Canadell, P. Ciais, P. Friedlingstein, F. Jotzo, D. P. van Vuuren, and C. L. Quéré, Nature Climate Change **4**, 873–879 (2014).

[3] C. McGlade, P. Ekins, Nature **517**, 187–190 (2015).

[4] G. Maggio, G. Cacciola, Fuel **98**, 111–123 (2012).

[5] A. E. Becquerel, Comptes Rendus de L'Académie des Sciences **9**, 145–149 (1839).

[6] D. M. Chapin, C. S. Fuller, and G. L. Pearson, J. Appl. Phys. **25**, 676 (1954).

[7] D. Meissner, in book: Materials and processes for energy: communicating current research and technological developments, Edition: Energy Book Series #1, Chapter: Photovoltaics Based on Semiconductor Powders, Publisher: Formatex Research Center, Badajoz, Spain, Editors: A. Méndez-Vilas, **126** (14) (2013).

[8] T. M. Clarke, J. Peet, P. Denk, G. Dennler, C. Lungenschmied, and A. J. Mozer, Energy Environ. Sci. **5**, 5241 (2012).

[9] N. Nekrašas, K. Genevičius, M. Viliūnas, G. Juška, Chem. Phys. **404**, 56–59 (2012).

[10] S. Bange, M. Schubert, D. Neher, Phys. Rev. B **81**, 035209 (2010).

[11] C. Deibel, A. Wagenpfahl, and V. Dyakonov, Phys. Rev. B **80**, 07520 (2009).

[12] A. Pivrikas, G. Juška, A. J. Mozer, M. Scharber, K. Arlauskas, N. S. Sariciftci, H. Stubb, and R. Österbacka, Phys. Rev. Lett. **94**, 176806 (2005).

[13] B. Philippa, M. Stolterfoht, R. D. White, M. Velusamy, P. L. Burn, P. Meredith, A. Pivrikas, J. Chem. Phys. **141**, 054903 (2014).

[14] P. Langevin, Ann. Chim. Phys. **28**, 433 (.1903).

[15] G. Juška, N. Nekrašas, K. Genevičius, J. Non-Cryst. Solids **358**, 748–750 (2012).

[16] D. H. K. Murthy, A. Melianas, Z. Tang, G. Juška, K. Arlauskas, F. Zhang, L. D. A. Siebbeles, O. Inganäs, T. J. Savenije, Adv. Funct. Mater. **23**, 4262–4268 (2013).

[17] A. J. Mozer, G. Dennler, N. S.. Westerling, A. Pivrikas, R. Österbacka, G. Juška, Phys. Rev. B **72,** 035217 (2005).

[18] R. Österbacka, A. Pivrikas, G. Juška, K. Genevičius, K.Arlauskas, and H. Stubb, Current Appl. Phys. **415**, 534–538 (2004).

[19] G. Juška, N. Nekrašas, V. Valentinavičius, P. Meredith, and A. Pivrikas, Phys. Rev. B **84,** 155202 (2011).

[20] A. Pivrikas, N.S. Sariciftci, G. Juška, R. Österbacka, Prog. Photovoltaics Res. Appl. **15** (8), 677–696 (2007).

[21] C. Deibel, A. Baumann, and V. Dyakonov, Appl. Phys. Lett. **93**, 163303 (2008).

[22] J. Peet, L. Wen, P. Byrne, S. Rodman, K. Forberich, Y. Shao, N. Drolet, R. Gaudiana, G. Dennler and D. Waller, Appl. Phys. Lett. **98**, 043301 (2011).

[23] G. Juška, K. Genevičius, N. Nekrašas, and G. Šliaužys, Phys. Status Solidi C **7** (3–4), 980–983 (2010).

[24] M. Koppe, H.-J. Egelhaaf, G. Dennler, M. C. Scharber, C. J. Brabec, P. Schilinsky, and C. N. Hoth, Adv. Funct. Mater. **20**, 338–346 (2010).

[25] M. Koppe, H.-J. Egelhaaf, E. Clodic, M. Morana, L. Lüer, A. Troeger, V. Sgobba, D. M. Guldi, T. Ameri, and C. J. Brabec, Adv. Energy Mater. **3**, 949–958 (2013).

[26] M. C. Scharber, M. Koppe, J. Gao, F. Cordella, M. A. Loi, P. Denk, M. Morana, H. J. Egelhaaf, K. Forberich, G. Dennler, R. Gaudiana, D. Waller, Z. Zhu, X. Shi, and C. J. Brabec, Adv. Mater. **22**, 367–370 (2010).

[27] G. Juška, N. Nekrašas, K. Arlauskas, J. Stuchlik, A. Fejfar, J. Kočka, Journal of Non-Crystalline Solids **338–340**, 353–356 (2004).

[28] J. Gorenflot, M. C. Heiber, A. Baumann, J. Lorrmann, M. Gunz, A. Kämpgen, V. Dyakonov, C. Deibel, J. Appl. Phys. **115,** 144502 (2014).

[29] C. G. Shuttle, R. Hamilton, J. Nelson, B. C. O'Regan, and J. R. Durrant, Adv. Funct. Mater. **20,** 698–702 (2010).

[30] A. V. Nenashev, M. Wiemer, A. V. Dvurechenskii, F. Gebhard, M. Koch, S. D. Baranovskii, Appl. Phys. Lett. **109,** 033301 (2016).

[31] J. Szmytkowski, Synth. Met. **206,** 120–123 (2015).

[32] D. Spoltore, W.D. Oosterbaan, S. Khelifi, J.N. Clifford, A. Viterisi, E. Palomares, M. Burgelman, L. Lutsen, D. Vanderzande, J. Manca, Adv. Energy Mater. **3** (4), 466–471 (2012).

[33] D. Rauh, C. Deibel, V. Dyakonov, Adv. Funct. Mater. **22,** 3371–3377 (2012).

[34] G. Juška, M. Viliūnas, and K. Arlauskas, Phys. Rev. B **51** (1995) 16668.

[35] G. J. Adriaenssens, V. I. Arkhipov, Solid State Commun. **103**, 541–543 (1997).

[36] L. J. A. Koster, V. D. Mihailetchi, and P. W. M. Blom, Appl. Phys. Lett. **88**, 052104 (2006).

Information about the author:

1. Name: Julius Važgėla.

2. Birth date: 1988-10-17.

3. Education:

2013-2017 doctoral studies (Vilnius University),

2011-2013 master degree studies (Vilnius University, Physical Technologies and Their Management),

2007-2011 bachelor degree studies (Vilnius University, Telecommunications Physics and Electronics),

4. Work experience:

2017 data analyst (Danske Bank),

2016-2017 junior researcher (Vilnius University, Department of Solid State Electronics),

2012-2016 technician (Vilnius University, Department of Solid State Electronics),

2013-2014 manager (JSC Amtest).

List of publications related to the thesis:

1. Julius Važgėla, Kristijonas Genevičius, Gytis Juška, I-CELIV technique for investigation of charge carriers transport properties, Chemical Physics **478**, 126–129 (2016), http://dx.doi.org/10.1016/j.chemphys.2016.04.005.
2. Julius Važgėla, Meera Stephen, Gytis Juška, Kristijonas Genevičius, Kęstutis Arlauskas, Charge Carrier Transport Properties in a Ternary Silole-Based Polymer:P3HT:PCBM Solar Cells, Lithuanian Journal of Physics **57** (1), 37–41 (2017), https://doi.org/10.3952/physics.v57i1.3454.
3. Julius Važgėla, Austėja Galvelytė, Gytis Juška, Mismatch of Bimolecular Recombination in Polymer TQ1/Fullerene Blends Employing Different Techniques, Organic Electronics **47**, 9–13 (2017), http://dx.doi.org/10.1016/j.orgel.2017.04.030.

List of presentations at the conferences (underlined Julius Važgėla – presented personally):

1. Meera Stephen, Julius Važgėla, Kristijonas Genevičius, Kęstutis Arlauskas, Gytis Juška, Charge Transport in Binary & Ternary Photo-Active Blends Probed via Electrical Methods, 6th International Summit on Organic Solar Cells (ISOS-6), Šamberi, Prancūzija, 2013.
2. Julius Važgėla, Meera Stephen, Gytis Juška, Kristijonas Genevičius, Kompozicijos įtaka organinių tūrinės heterosandūros saulės elementų krūvininkų judriui bei rekombinacijai, Tarpdalykiniai tyrimai fiziniuose ir technologijos moksluose – 2014, Vilnius, 2014.
3. Kristijonas Genevičius, Nerijus Nekrašas, Gytis Juška, Julius Važgėla, Giedrius Juška, Meera Stephen, I-CELIV Method for Investigation of Charge Carriers Mobilities and Interface Recombination, ESOS – European Summer School on Organic Photovaltaic Stability, Kargesas, Prancūzija, 2015.

4. Julius Važgėla, Gytis Juška, Low Band Gap Polymer PCPDTBT:$PC_{61}BM$ Bulk Heterojunction Solar Cells Investigated by MIS-CELIV technique, Functional Materials and Nanotechnologies, Vilnius, 2015.

5. Julius Važgėla, Gytis Juška, Kristijonas Genevičius, Charge Carrier Transport Studies with i-CELIV Method, Tarpdalykiniai tyrimai fiziniuose ir technologijos moksluose – 2016, Vilnius, 2016.

6. Julius Važgėla, Kristijonas Genevičius, Gytis Juška, Charge Carriers Transport Properties in PCBM:PCPDTBT Bulk Heterojunction investigated by i-CELIV technique, International Symposium for the 80th Birthday of Prof. Alan J. Heeger, Lincas, Austrija, 2016.

7. Julius Važgėla, Kristijonas Genevičius, Gytis Juška, I-CELIV Technique for Charge Carriers Transport Studies, E-MRS Spring Meeting, Lilis, Prancūzija, 2016.

8. Julius Važgėla, Meera Stephen, Gytis Juška, Kristijonas Genevičius, Kęstutis Arlauskas, Reduced Bimolecular Recombination in a Ternary Silole-Based Polymer:P3HT:PCBM Solar Cell, IV Lithuanian-Ukrainian-Polish Meeting on Physics of Ferroelectrics, Palanga, 2016.

9. Julius Važgėla, Austėja Galvelytė, Gytis Juška, Mismatch of Non-Geminate Recombination in Polymer TQ1/Fullerene Blends Employing Different Techniques, HOPV 17, Lozana, Šveicarija, 2017.